Article

Not peer-reviewed version

Design and Utilization of a 3D printed Tooth-Borne Orthodontic Molar Distalizer Library

Bregt Smeets * and Tim Smeets

Posted Date: 6 February 2024

doi: 10.20944/preprints202401.2047.v2

Keywords: distalizer; orthodontics; digital; biocompatible 3D printing; dental biocompatible resin; CAD/CAM; computer modelling; class II; molar derotation

Preprints.org (www.preprints.org) | NOT PEER-REVIEWED | Posted: 6 February 2024 doi:10.20944/preprints202401.2047.v2

Article

Design and Utilization of a 3D Printed Tooth-Borne Orthodontic Molar Distalizer Library

Bregt Smeets [1,†,‡], and Tim Smeets [2,‡,§]

[1] PgO UCAM; bregt.smeets@prodentatech.be
[2] K.U. Leuven; tim.smeets@student.kuleuven.be
* Correspondence: bregt.smeets@prodentatech.be; Tel.: +32-472-281618
† 3D Design, 3D printing and Clinical work
‡ Data Analysis
§ Statistical Analysis

Abstract: This papers' objective is to describe a method of in-office 3D designing and 3D printing a tooth-borne molar distalizer and create a library, to easily reproduce the needed distalizers, in a private orthodontic clinic. Research objectives were to design and 3D print molar distalizers, clinically use in orthodontic treatment settings, assess the strength and frequency of debonding and or breakage. The print resin used was Dental LT Clear V2 (RS-F2-DLCL-02) from formlabs. The 3D printer used was a Formlabs 3B+printer. 16 patients were treated with these 3D printed distalizers. Patients selected were between 11 Years and 49 Years old, Class II occlusion with no skeletal Class II values. The skeletal cephalometric values of the six patients were within the range of SNA = 81± 3° , SNB = 78 ± 3° , ANB = 3 ± 2°. The mean duration of the 3D printed appliance was 14.58 ± 4.31 weeks. The aim reached, was to position molars and canines in a dental Class I position. The combined failure rate was 0.94. A library of distalizers has been made of sizes between 16mm and 29mm, they are easy to print and easy to use in office.

Keywords: distalizer; orthodontics; digital; biocompatible 3D printing; dental biocompatible resin; CAD/CAM; computer modelling; class II; molar derotation.

---

1. Introduction

In recent years 3D printing technology endured significant technological improvements[1–10]. Whereas SLA, DLP and LCD based 3D printers improved[6,7,10–14], 3D printing resins proved to be bio-compatible[3,9,12,14–18] and being able to endure masticatory forces[5,8,11,14,18–20]. This enabled orthodontists to set up their own 3D lab and design and print a variety of orthodontic appliances. Molar distalizers exist in a variety of solutions. As there are appliances as Hilgers pendulum[21], distal jet appliance[22], modified slider[23], intraoral bodily molar distalizer[24], J-Molar Distalizer[25], Greenfield lingual distalizer[26] or simplified molar distalizer[27], which are fixed appliance connected to a plastic pad in contact with the palatal ruggae, with springs or rotary devices to distalize molars. These have the disadvantage of disto-rotating the mandible thus increasing the anterior facial height[28, 29]. Others like the Hybrid hyrax Distalizer are printed in metal, and skeletally anchored in the palate with the use of mini-implants, thus avoiding the disto-rotation of the mandible [30,31]. The appliance proposed in this article is an in office designed distalizer comparable to Carriere® Motion 3D™ (Henry Schein Orthodontics, Carlsbad, Ca, USA)[1,32–46], consisting of a rigid bar connected with a pad on the canine attached to the anterior third of the clinical crown, with a mesial hook attached to it and pivoting in a ball-and-socket joint with a pad bonded to center of the clinical crown of molar facilitating the distalization en derotation of the molar. The activation of the device is done with elastics attached to the medial hook on the canine. Measuring the results are shown using CBCT [37,45,47,48], cephalometric superimposition and model [1,49] or overlay of the STL files before and after treatment [1,35]. The advantage of using a distalizer is its insertion at the beginning of the treatment, when compliance is still high. A distalizer is a low invasive, with easy placement and removal technique

Preprints.org (www.preprints.org) | NOT PEER-REVIEWED | Posted: 6 February 2024 doi:10.20944/preprints202401.2047.v2

advantages. The doughnut in a socket design on the molar pad is tipping and derotation the upper first molar. The hook on the canine pad allows Class II elastics to be worn attached to the lower first or second molar [32].

2. Materials and Methods

1. Digital Design

Digital bio-compatible Additive Manufacturing (AM), brings 3D printing and manufacturing closer to a orthodontic practice, and allows for manufacturing of distalizers, power-arms, retainers and other perceivable orthodontic auxiliaries[14,17,18,50] .

The bio-compatible resin chosen, Dental LT Clear, has been applied with success in orthodontic manufacturing [3,5,8,9,11,12,18,20,50]. For 3D printing we opted for a Formlabs 3B+ printer. There has been extensive research comparing 3D print technology [4,6,7,10,12–14,51]. These conclude that model position [13], anti-aliasing, grey-scale and blur [7,52] are the most influencing parameters. Positioning parallel to the 3D printer tray [14] is favourable and we used the anti-aliasing, grey-scale and blur settings proposed by the manufacturer.

We start the design process with drawing a cylinder with the desired shape, we design a spline to sweep the cylinder over to form the arm. Finally we make the rotary part of the molar hinge Figure 1. This concise of a sphere with a diameter of 2.52mm, here we make indentations on the side of this ball with spheres with diameter 10mm. These indentations will allow the arm to click in place in the molar base. The software used is Fusion360 and 123D Design both from Autodesk™[53].

Figure 1. First a cylinder is swept over a preformed spline to form the arm, the cylinder is then cut away. Lastly a flattened sphere is formed as part of the hinge.

Form a hemisphere with the desired size and attach to the arm to form the canine attachment Figure 2. Another hemisphere is being created on top of the canine attachment to create the hook for the elastics. A cutout is made with a round edged box and finally the top edge of the cutout has been rounded off Figure 3.

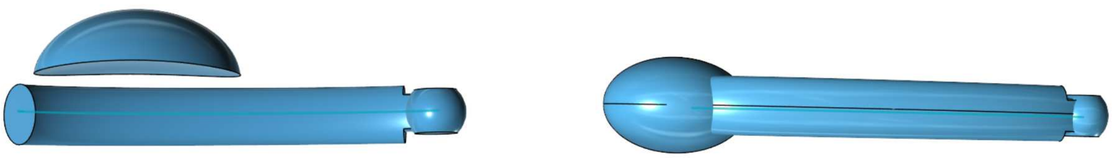

Figure 2. A hemi-sphere is added to form the canine or premolar attachment

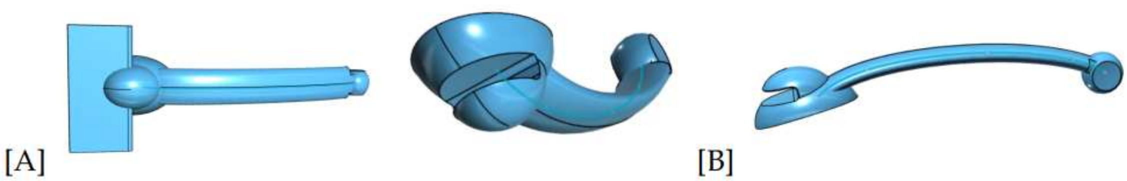

Figure 3. (**A**). Another hemisphere is being added and the elastic attachment is being formed, a cut-out is made with a round edged box. (**B**). The upper edge of the thus resulting hook is rounded off.

Preprints.org (www.preprints.org) | NOT PEER-REVIEWED | Posted: 6 February 2024 doi:10.20944/preprints202401.2047.v2

We start with a hemisphere ⌀ 7.5mm to form the molar attachment. The molar pad will be flattened on the side and a large sphere ⌀ 35mm is used to form the concavity of of the molar pad. Then a cutout is made first in 90º then a second cutout in -18º Figure 4. A copy of the existing arm is enlarged 1.1 and used to make the cutout in the molar pad. After this the entrance is enlarged to facilitate the rotation of the arm Figure 5.

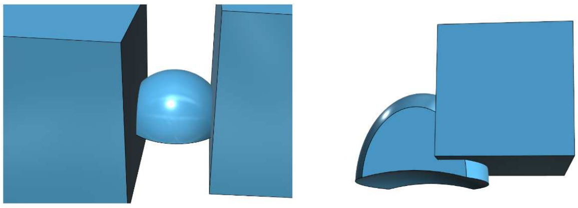

Figure 4. Flattening the side of the hemisphere and preparing the cutout.

[A] [B]

Figure 5. (**A**). With the arm 1.1 time enlarged prepare the cutout in the molar pad. (**B**). Make a cutout to allow the rotation of the arm in the molar pad.

In Figure 6A the completed molar hinge is shown. In Figure 6B the completed arm is shown.

[A] [B]

Figure 6. (**A**). The finished molar pad. (**B**). The finished distalizer.

2. Patient Selection

Patients were chosen by the following selection criteria:

1. Class II occlusion with no skeletal Class II values
2. Skeletal cephalometric values of SNA = 81± 3º , SNB = 78 ± 3º , ANB = 3 ± 2º ;
3. Patients were compliant with dental monitoring on a monthly basis;

3. Printing

The bio-compatible resin chosen, Dental LT Clear, has been applied with success in orthodontic manufacturing [3,5,8,9,11,12,17,18,20]. For 3D printing we opted for a Formlabs™Form 3B+ , as it has been validated in FDA-cleared workflows. There has been extensive research comparing 3D print technology [4,6,7,10,12–14,51,54,55]. These conclude that model position [9,13], anti-aliasing, grey-scale and blur [7,52] are the most influencing parameters. Positioning parallel to the 3D printer tray [14] is favourable and we used the anti-aliasing, grey-scale and blur settings proposed by the manufacturer.

 doi:10.20944/preprints202401.2047.v2

4. Post-Processing after 3D Printing

After printing the distalizer Figure 7, it must be washed, and the support removed. We used a FormWash filled with a concentration of 99% IPA, to comply with bio-compatibility regulations [56]. 3D printed parts require post processing in order to ensure their optimal performance and bio-compatibility of the 3D printed dental appliances. Parts 3D printed with the Dental LT Clear V2 Resin should be first washed for 15 minutes, then soaked in fresh isopropyl alcohol for the remaining 5 minutes. Leaving the parts in the IPA for longer than 20 minutes will result in lower quality of the parts due to excessive solvent exposure[56].

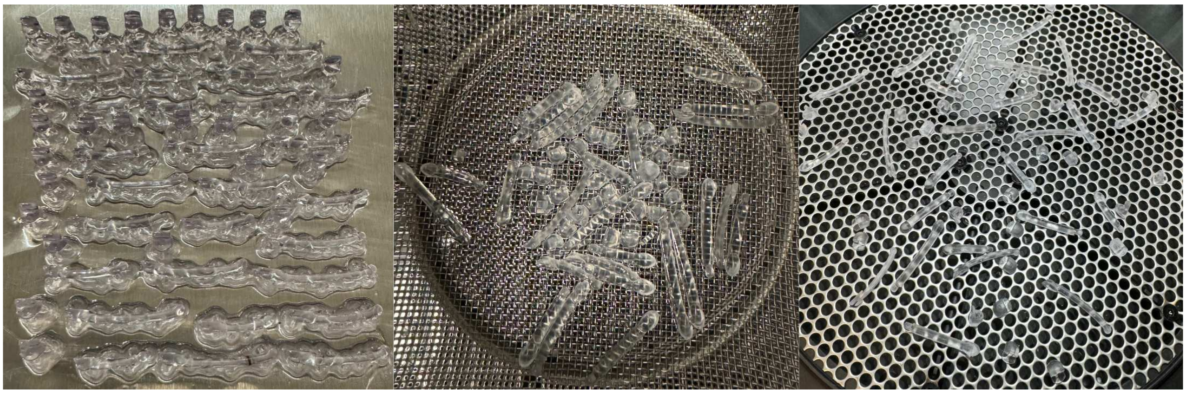

Figure 7. The distalizers on the print plate; the distalizers in the washer; the distalizers after post cure.

Curing was done with the help of the FormCure curing chamber (60 minutes at 60 ºC).This cure setting ensures that it achieves both bio-compatibility and optimum mechanical properties Figure 8 [57].

Figure 8. Motions in sizes 16-29mm, after curing.

5. Testing

We build testing equipment to test the distalizers resistance to force. The first tool was a jaw that could open and close, this each time 1200 cycles and this repeated as much as needed. Software was

 doi:10.20944/preprints202401.2047.v2

written for an arduino uno with a LCD screen and keypad, the moving force was produced through a servo motor. The whole tool was 3D printed with a Ultimaker 3 and PETG filament. The upper jaw in the tool had places prepared to glue human teeth into. Two human teeth were bonded to the tool, and the distalizer attached to them. Figure 9.

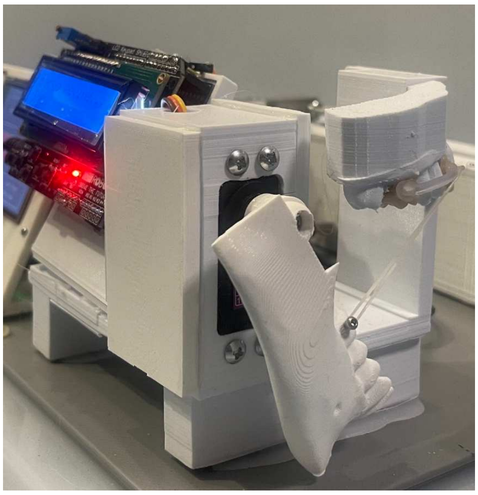

Figure 9. 3D printed cyclic distalizer tester.

The second testing tool was built using an Arduino Mega and a touchscreen. The software used to drive this was written by ourselves. A stepper motor and stepper motor driver board were being attached. A worm drive was connected to the stepper motor, moving a sled on which the distalizer was attached. A load-cell of 10kg was used to measure the maximum load applied using 1/4' 6oz. and 1/4' 8oz. elastics Figure 10. The tool was 3D printed with a Ultimaker 3 with peg filament. No distalizers were damaged using this testing process.

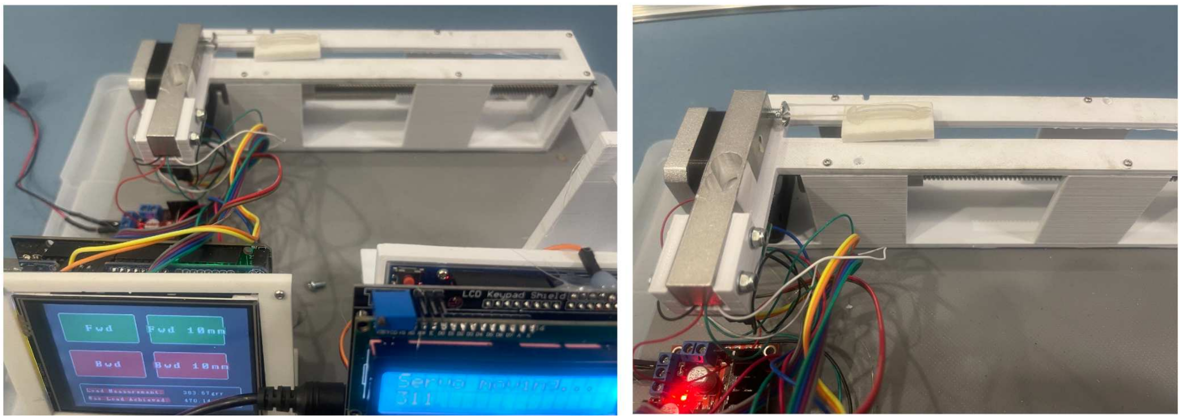

Figure 10. 3D printed strain tester.

6. Clinical Application

The 3D printed distalizers were prepared, sandblasting the canine and molar bonding pads. Then Transbond™ XT (3M Unitek)primer was applied to the pads and light cured [58]. Transbond™ XT (3M Unitek) light cure paste was used to bond the distalizer to the teeth, after the teeth were cleaned, etched and Transbond™ XT (3M Unitek) primer applied [59]. Before light curing excessive remnants were being removed. The activation of the molar distalizers was done with class II elastics, during testing from beginning until the end with 1/4 inch (6.35mm), 6 oz (170 g) elastics were connected from the canine pad to a button on teeth 46 or 47 and 36 or 37 [60–63].

7. Measurements The 3D scans were made with the 3Shape TRIOS® 4 and measurements were done within the software of Medit-Link with the Medit design app (©MEDIT corp. 8, Yangpyeong-ro

Preprints.org (www.preprints.org) | NOT PEER-REVIEWED | Posted: 6 February 2024 doi:10.20944/preprints202401.2047.v2

25-gil, Yeongdeungpo-gu, Seoul, Republic of Korea) [64,65]. The measurements were done independent by 2 researchers, each two times with 7 days between both measurements. The distalisation was measured on an overlay of the STL-file at the beginning and at the end, where a fixed point on the canines and molars in both STL's was used. A line connecting respectively canines and molars was drawn on which the same point on canines and molars in the overlay STL were measured in distance perpendicular to the lines in the first STL.

The derotation was measured by comparison of the angulation of a line between distinct point on the vestibular side and a distinct point on palatal side, wereas each researcher decided independently [35,46,49].

3. Results

The objective was to propose a method of designing a molar distalizer library, and forthcoming manufacture the molar distalizers in-office as described in the digital-design part.

The next objective was the evaluation of failure, both breakage and debonding and thus evaluating the relative strength in vivo.

Table 1 shows the overview of 16 patients treated with these 3d printed molar distalizers. Assuming a moderate effect (d = 0.7) and a alpha error of 0.05, the sample size calculation using the G-Power analysis yields a total sample size of n = 13. In this table we list the age of participating patients, the time the distalizers have been worn, the size of distalizers used and the failure rate.

We add Table 2 for descriptive purpose. We see an age span between 11-49 years of age, a range of distalizers between 18 and 27mm. The short distalizers are those bonded from premolar to molar, the longer ones ($\geq 24mm$) bonded from canine to molar. The time needed to achieve a molar Class I was on average 14.6 weeks, with a total failure rate, left and right distalizer per patient combined, of 94%. On average, we see a breakage of one distalizer, left or right, per patient. The failures were breakage of the arm at the canine pad.

Table 1. Results of clinical evaluation.

ID	Age in Decimals	Time Worn	Size Right	Size Left	Failure	Failure
#	[years]	[weeks]	[mm]	[mm]	#	#
1	14.95	16.71	25	25	0	0
2	14.95	16.71	25	25	1	0
3	12.62	11.57	25	25	0	0
4	15.41	17.71	26	27	1	0
5	11.74	17.57	26	26	0	1
6	14.28	9.14	24	25	0	0
7	17.91	13.57	24	24	0	0
8	49.34	14.00	26	26	1	1
9	12.94	11.29	19	19	1	1
10	14.92	17.14	27	27	1	1
11	14.11	10.00	26	26	0	1
12	11.89	24.86	26	26	1	0
13	15.41	10.29	25	25	1	1
14	14.06	19.57	24	25	0	0
15	13.07	9.86	18	18	0	0
16	15.34	13.29	24	24	0	1

Preprints.org (www.preprints.org) | NOT PEER-REVIEWED | Posted: 6 February 2024 doi:10.20944/preprints202401.2047.v2

Table 2. Descriptive analysis.

Variable	Statistics or Category	Values
Age [years]	mean ± SD [1]	16.43 ± 8.91
	median (range)	14.60 (11.74 - 49.34)
Size [mm]	median (range)	25.00 (18.00 - 27.00)
Time worn [weeks]	mean ± SD	14.58 ± 4.31
	median (range)	13.79 (9.14 - 24.86)
Total failures [2]	mean	0.94

[1] SD: standard deviation. [2] Data of left and right distalizers combined for each individual patient

The results are shown using overlay of the STL files before and after treatment [1,35].

The overlay results of the 3D scans show the distalisation and derotation Figure 11.

A high correlation was found between the derotation values of the left upper molar and the right upper molar (ρ = 0.713; p = 0.002) (Figure 13C). There is no correlation between the right upper molar distalization and the left upper molar distalization values (ρ = 0.214; p = 0.426) (Figure 13B). There was a high correlation found between the right upper canine distalization values and the right upper molar distalization values (ρ = 0.789; p = <0.001) (Figure 12C), even though no correlation could be found between distalization values of the left upper canine and the left upper molar (ρ = 0.417; p = 0.108) (Figure 12D). No correlation could be found between the displacement value of the upper left molar and it's derotation angle (ρ = 0.139; p = 0.608) (Figure 12B), and a high correlation could be found between the displacement of the upper right molar and it's derotation angle (ρ = 0.765; p = <0.001) (Figure 12A). There is a high correlation between the right upper canine distalization and the left upper canine distalization values (ρ = 0.630; p = 0.009) (Figure 13A).

Preprints.org (www.preprints.org) | NOT PEER-REVIEWED | Posted: 6 February 2024 doi:10.20944/preprints202401.2047.v2

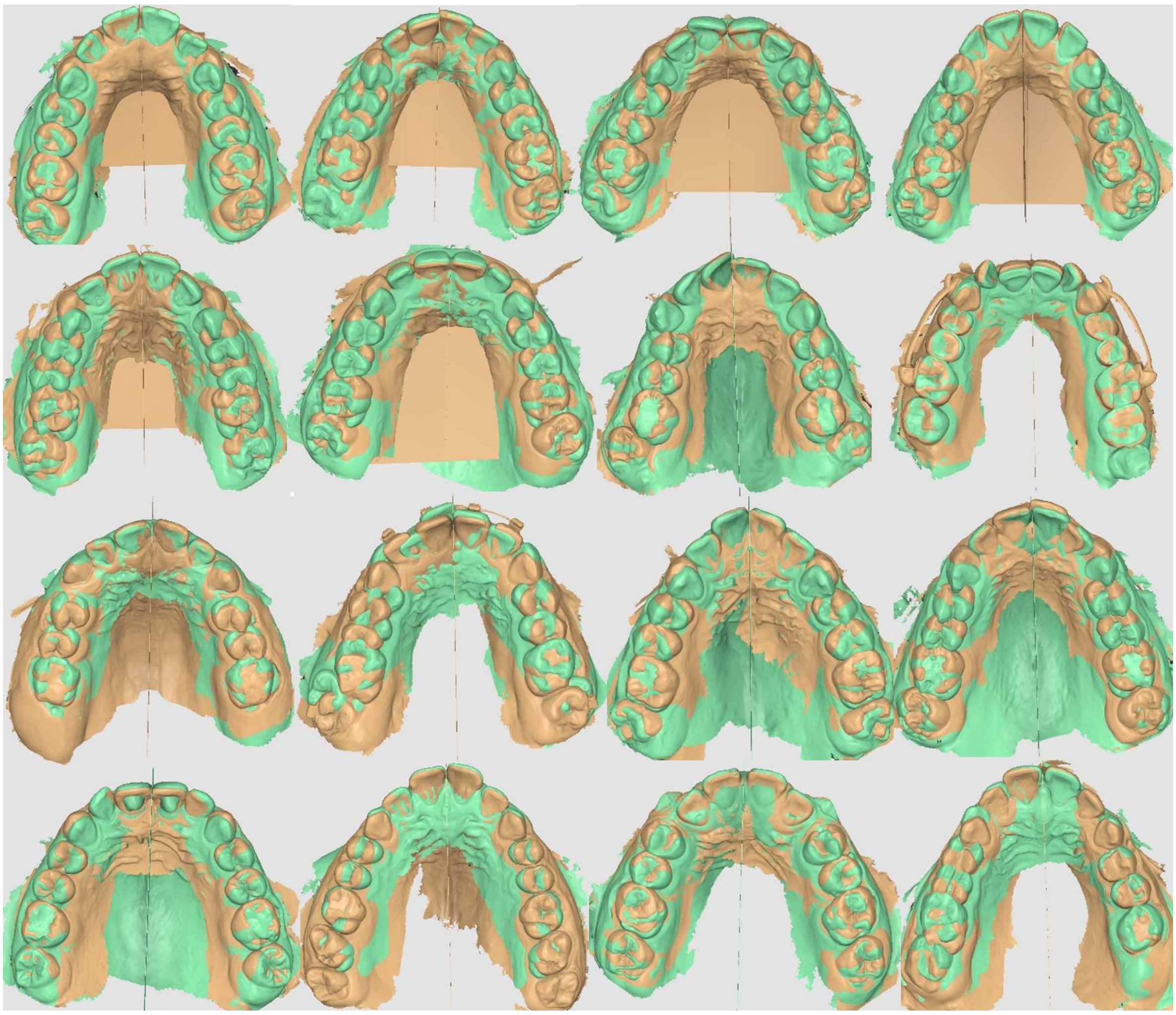

Figure 11. The overlays of the 16 patients.

Intraclass correlation coefficients (ICC) showed good interindividual and intraindividual agreement (interindividual: mean ICC: 0.95, range: 0.93 - 0.98; intraindividual: mean ICC: 0.99, range: 0.990-0.993)

Table 3. Descriptive statistics of the distal tooth displacement, left and right, of the upper canines (mm), upper first molars (mm), and the derotation angle of the upper first molars (°).

	Mean	SD [1]	Minimum	Maximum
Left upper canine displacement	3.054	1.476	0.88	7.06
Right upper canine displacement	3.620	1.471	1.24	6.63
Left upper molar displacement	2.597	1.565	0.82	7.06
Right upper molar displacement	2.333	1.097	0.83	4.21
Left upper molar derotation angle	5.711	4.488	0.58	15.98
Right upper molar derotation angle	6.484	4.108	0.63	16.08

[1] SD: standard deviation

Preprints.org (www.preprints.org) | NOT PEER-REVIEWED | Posted: 6 February 2024 doi:10.20944/preprints202401.2047.v2

Table 4. Descriptive statistics of the distal tooth displacement of upper canines (mm), upper first molars (mm), and the derotation angle of the upper first molars (°).

	n	Mean	SD [1]	Minimum	Maximum
Upper canine displacement	32	3.157	1.453	0.88	7.06
Upper molar displacement	32	2.465	1.336	0.82	7.06
Upper molar derotation angle	32	6.098	4.250	0.58	16.08

[1] SD: standard deviation

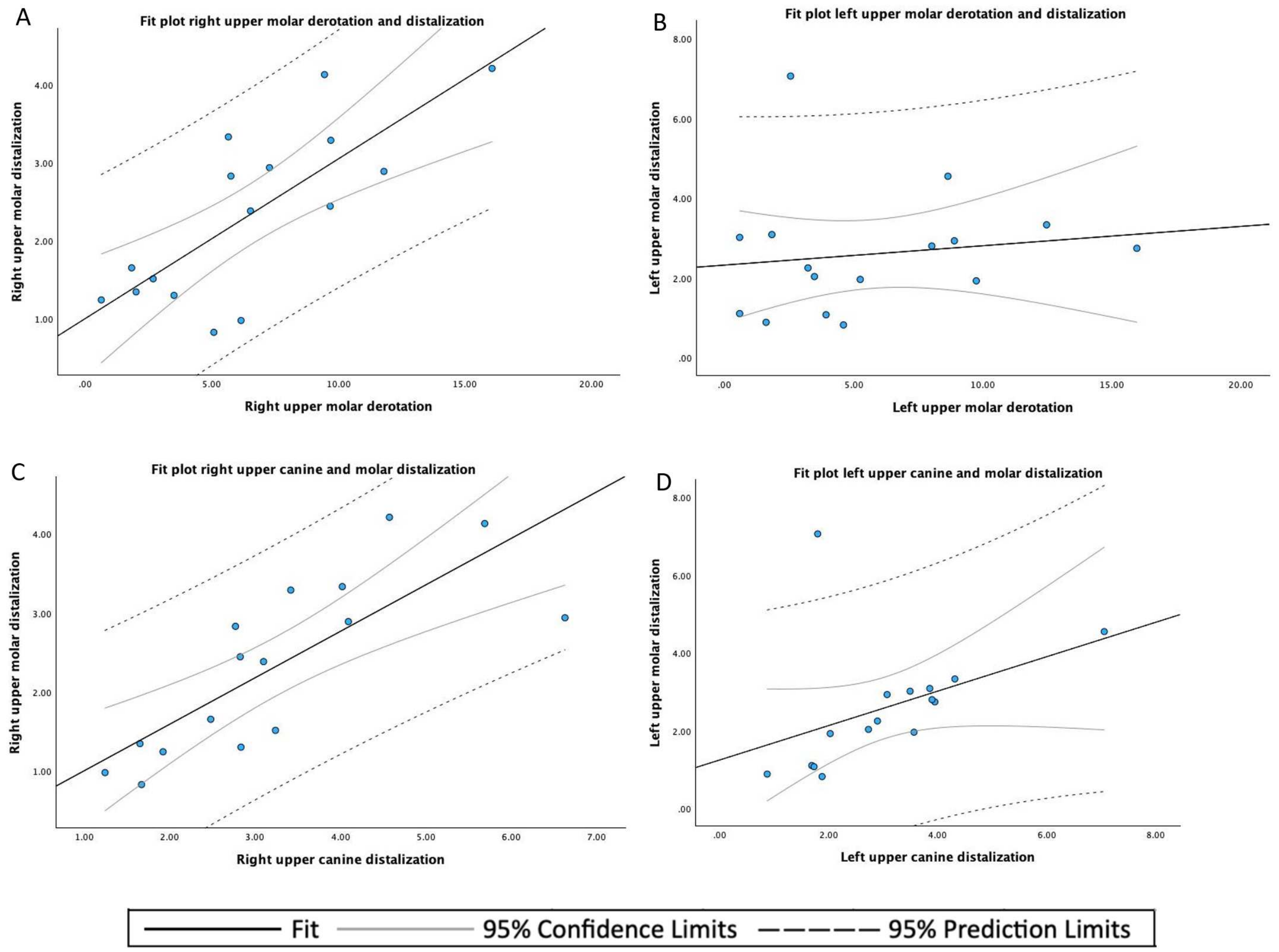

Figure 12. (**A**) Fit plot of right upper molar derotation and distalization; (**B**) Fit plot of left upper molar derotation and distalization; (**C**) Fit plot of right upper canine and molar distalization; (**D**) Fit plot of left upper canine and molar distalization

Preprints.org (www.preprints.org) | NOT PEER-REVIEWED | Posted: 6 February 2024 doi:10.20944/preprints202401.2047.v2

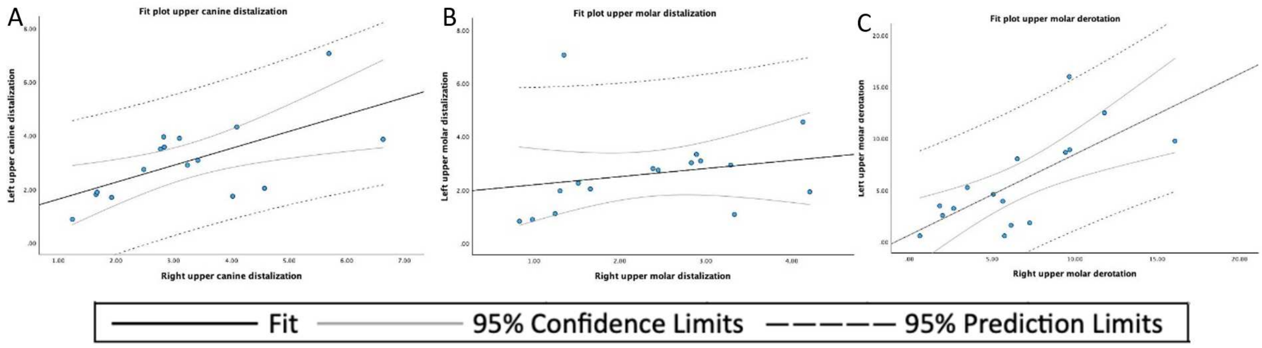

Figure 13. (**A**) Fit plot of the upper canine distalization; (**B**) Fit plot of the upper molar distalization; (**C**) Fit plot of the upper molar derotation

4. Discussion

The proposed method of 3D designing and 3D printing is just a new step in in-office designing and manufacturing of orthodontic devices. Fusion 360 generative design and Finite Elements Analysis, aid in designing with the use of artificial intelligence. More data of actual forces applied on distalizers, is needed to be able to build a reliable mathematical model, thus improving artificial intelligence and facilitating Additive Manufacturing. The 3D dental printers and biocompatible 3D printing resins available, facilitate the manufacturing in-office [2,12,14,51]. Even though breakage and debonding incidents were noted, they were caused by patient-admitted non-compliance during eating. Due to the transparency of the material, easy bonding by light curing was achieved. Even the replacement of a broken arm of the distalizer was fast by, after removing the remains of the broken arm, clicking the new arm in the existing molar pad and rebonding the canine or premolar pad. The results presented show a proof of concept. Further research will be done to reduce breakage of the presented molar distalizers.

5. Conclusions

The results show the creation of a library of 3D printed distalizers, sizes 16-29mm. There was an acceptable failure rate and yet distalization and derotation capabilities comparable to CMA [1,32,33,35, 40,41,43–46,48–50,66].

Author Contributions: Conceptualization, S.B. ; methodology, S.B.; software, S.B. and S.T.; validation, S.B.and S.T.; formal analysis, S.B. and S.T..; investigation, S.B.; resources, S.B.; data curation, S.B. and S.T.; writing—original draft preparation, S.B..; writing—review and editing, S.B.; visualization, S.B. and S.T.; supervision, S.B.; project administration, S.B.. Both authors have read and agreed to the published version of the manuscript."

Funding: No funding, grants or other support was received

Institutional Review Board Statement: The study was conducted according to the guidelines of the Declaration of Helsinki, no approval was necessary by the Ethics Committee. Ethical review and approval were waived for this study, due to the fact that no experimental materials or approaches were used. All used materials are fully certified and are available in the market. Dental LT Clear (V2) is certified as bio-compatible per EN-ISO 10993-1:2009/AC:2010. The bio-compatible resin material follows ISO Standards: EN-ISO 1641:2009, EN-ISO 10993-1:2009/AC:2010, EN-ISO 10993-3:2009, EN-ISO 10993-5:2009, EN 908:2008.Formlabs electrical equipment is manufactured in facilities with the following QMS certifications. Form 3B+ (Quality system standards) ISO 9001:2015 and ISO 14001:2015.

Informed Consent Statement: Written informed consent was obtained from all subjects involved in this study.

Data Availability Statement: Data available in a publicly available repository, this data is available here [https://drive.google.com/drive/folders/1ASH5q6cuZN6bNKHy_dzt_xntl5_JRNkM?usp=sharing]

Acknowledgments: We acknowledge the support of Tandartsenpraktijk ProDenta BV for the use of the lab infrastructure.

Conflicts of Interest: The authors declare no conflicts of interest.

Abbreviations

The following abbreviations are used in this manuscript:

MDPI	Multidisciplinary Digital Publishing Institute
DOAJ	Directory of open access journals
CMA	Carriere motion appliance
AM	Additive Manufacturing
ICC	Intraclass Correlation Coefficients

References

1. Schmid-Herrmann, C.U.; Delfs, J.; Mahaini, L.; Schumacher, E.; Hirsch, C.; Koehne, T.; Kahl-Nieke, B. Retrospective investigation of the 3D effects of the Carriere Motion 3D appliance using model and cephalometric superimposition. *Clin Oral Investig* **2023**, *27*, 631–643. https://doi.org/10.1007/s00784-022-04768-4.
2. Eliades, T.; Zinelis, S. Three-dimensional printing and in-house appliance fabrication: Between innovation and stepping into the unknown. *Am J Orthod Dentofacial Orthop* **2021**, *159*, 1–3. https://doi.org/10.1016/j.ajodo.2020.10.012.
3. Tartaglia, G.M.; Mapelli, A.; Maspero, C.; Santaniello, T.; Serafin, M.; Farronato, M.; Caprioglio, A. Direct 3D printing of clear orthodontic aligners: Current state and future possibilities. *Materials* **2021**, *14*, 1799. https://doi.org/10.3390/ma14071799.
4. Jiang, T.; Yan, B.; Jiang, M.; Xu, B.; Xu, Y.; Yu, Y.; Ma, T.; Wang, H. Enhanced Adhesion-Efficient Demolding Integration DLP 3D Printing Device. *Applied sciences* **2022**, *12*, 7373. https://doi.org/10.3390/app12157373.
5. Paradowska-Stolarz, A.; Malysa, A.; Mikulewicz, M. Comparison of the Compression and Tensile Modulus of Two Chosen Resins Used in Dentistry for 3D Printing. *Materials* **2022**, *15*, 8956. https://doi.org/10.3390/ma15248956.
6. Tsolakis, I.A.; Papaioannou, W.; Papadopoulou, E.; Dalampira, M.; Tsolakis, A.I. Comparison in Terms of Accuracy between DLP and LCD Printing Technology for Dental Model Printing. *Dentistry journal* **2022**, *10*, 181. https://doi.org/10.3390/dj10100181.
7. Montgomery, S.M.; Demoly, F.; Zhou, K.; Qi, H.J. Pixel-Level Grayscale Manipulation to Improve Accuracy in Digital Light Processing 3D Printing. *Advanced functional materials* **2023**. https://doi.org/10.1002/adfm.202213252.
8. Paradowska-Stolarz, A.; Wieckiewicz, M.; Kozakiewicz, M.; Jurczyszyn, K. Mechanical Properties, Fractal Dimension, and Texture Analysis of Selected 3D-Printed Resins Used in Dentistry That Underwent the Compression Test. *Polymers* **2023**, *15*, 1772. https://doi.org/10.3390/polym15071772.
9. Revilla-León, M.; Cascos-Sánchez, R.; Zeitler, J.M.; Barmak, A.B.; Kois, J.C.; Gómez-Polo, M. Influence of print orientation and wet-dry storage time on the intaglio accuracy of additively manufactured occlusal devices. *The Journal of prosthetic dentistry* **2023**. https://doi.org/10.1016/j.prosdent.2022.12.005.
10. Vlasa, A.; Bocanet, V.I.; Muntean, M.H.; Bud, A.; Dragomir, B.R.; Rosu, S.N.; Lazar, L.; Bud, E. Accuracy of Three-Dimensional Printed Dental Models Based on Ethylene Di-Methacrylate-Stereolithography (SLA) vs. Digital Light Processing (DLP). *Applied sciences* **2023**, *13*, 2664. https://doi.org/10.3390/app13042664.
11. Marcel, R.; Reinhard, H.; Andreas, K. Accuracy of CAD/CAM-fabricated bite splints: milling vs 3D printing. *Clinical oral investigations* **2020**, *24*, 4607–4615. https://doi.org/10.1007/s00784-020-03329-x.
12. Barone, S.; Neri, P.; Paoli, A.; Razionale, A.V.; Tamburrino, F. Development of a DLP 3D printer for orthodontic applications. *Procedia Manufacturing* **2019**, *38*, 1017–1025. https://doi.org/10.1016/j.promfg.2020.01.187.
13. Yao, L.; Hu, P.; Wu, Z.; Liu, W.; Lv, Q.; Nie, Z.; Zhengdi, H. Comparison of accuracy and precision of various types of photo-curing printing technology. *Journal of Physics: Conference Series* **2020**, *1549*, 32151. https://doi.org/10.1088/1742-6596/1549/3/032151.
14. Farkas, A.Z.; Galatanu, S.V.; Nagib, R. The Influence of Printing Layer Thickness and Orientation on the Mechanical Properties of DLP 3D-Printed Dental Resin. *Polymers* **2023**, *15*, 1113. https://doi.org/10.3390/polym15051113.

15. Schuster, M.; Turecek, C.; Mateos, A.; Stampfl, J.; Liska, R.; Varga, F. Evaluation of Biocompatible Photopolymers II: Further Reactive Diluents. *Monatshefte fur Chemie* **2007**, *138*, 261–268.
16. Alifui-Segbaya, F.; Varma, S.; Lieschke, G.; George, R. Biocompatibility of Photopolymers in 3D printing. *Addit. Manuf.* **2017**, *4*, 185–191.
17. Thurzo, A.; Sufliarsky, B.; Urbanova, W.; Cverha, M.; Strunga, M.; Varga, I. Pierre Robin Sequence and 3D Printed Personalized Composite Appliances in Interdisciplinary Approach. *Polymers* **2022**, *14*, 3858. https://doi.org/10.3390/polym14183858.
18. Goracci, C.; Juloski, J.; D'Amico, C.; Balestra, D.; Volpe, A.; Juloski, J.; Vichi, A. Clinically Relevant Properties of 3D Printable Materials for Intraoral Use in Orthodontics: A Critical Review of the Literature. *Materials* **2023**, *16*, 2166. https://doi.org/10.3390/ma16062166.
19. Chen, S.; Yang, J.; Jia, Y.G.; Lu, B.; Ren, L. Study of a 3D-Printable Reinforced Composite Resin: PMMA Modified with Silver Nanoparticles Loaded Cellulose Nonocrystal. *Materials* **2018**, *11*.
20. Aretxabaleta, M.; Xepapadeas, A.B.; Poets, C.F.; Koos, B.; Spintzyk, S. Fracture load of an orthodontic appliance for robin sequence treatment in a digital workflow. *Materials* **2021**, *14*, 1–17. https://doi.org/10.3390/ma14020344.
21. Hilgers, J.J. The pendulum appliance for Class II non-compliance therapy. *J Clin Orthod* **1992**, *26*, 706–14.
22. Kinzinger, G.S.; Diedrich, P.R. Biomechanics of a Distal Jet appliance. Theoretical considerations and in vitro analysis of force systems. *Angle Orthod* **2008**, *78*, 676–81. https://doi.org/10.2319/0003-3219(2008)078[0676:BOADJA]2.0.CO;2.
23. Sayinsu, K.; Isik, F.; Allaf, F.; Arun, T. Unilateral molar distalization with a modified slider. *European journal of orthodontics* **2006**, *28*, 361–365. https://doi.org/10.1093/ejo/cji118.
24. Keles, A.; Sayinsu, K. A new approach in maxillary molar distalization: Intraoral bodily molar distalizer. *American journal of orthodontics and dentofacial orthopedics* **2000**, *117*, 39–48. https://doi.org/10.1016/S0889-5406(00)70246-0.
25. Batra, P.; Ragini, R. The J-Molar Distalizer for bodily molar movement. *Journal of clinical orthodontics* **2014**, *48*, 312–315.
26. Greenfield, R.L. The Greenfield lingual distalizer. *Journal of clinical orthodontics* **2005**, *39*, 548–56; quiz 532.
27. Walde, K.C. The simplified molar distalizer. *Journal of clinical orthodontics* **2003**, *37*, 616–9; quiz 626.
28. Ghosh, J.; Nanda, R.S. Evaluation of an intraoral maxillary molar distalization technique. *Am J Orthod Dentofacial Orthop* **1996**, *110*, 639–46. https://doi.org/10.1016/s0889-5406(96)80041-2.
29. Byloff, F.K.; Darendeliler, M.A.; Clar, E.; Darendeliler, A. Distal molar movement using the pendulum appliance. Part 2: The effects of maxillary molar root uprighting bends. *Angle Orthod* **1997**, *67*, 261–70. https://doi.org/10.1043/0003-3219(1997)067<0261:DMMUTP>2.3.CO;2.
30. Clarenbach, T.H.; Wilmes, B.; Ihssen, B.; Vasudavan, S.; Drescher, D. Hybrid hyrax distalizer and mentoplate for rapid palatal expansion, class III treatment, and upper molar distalization. *Journal of clinical orthodontics* **2017**, *51*, 317–325.
31. Graf, S.; Vasudavan, S.; Wilmes, B. CAD/CAM Metallic Printing of a Skeletally Anchored Upper Molar Distalizer. *Journal of clinical orthodontics* **2020**, *54*, 140–150.
32. Carrière, L. A new Class II distalizer. *Journal of clinical orthodontics* **2004**, *38*, 224–231.
33. Luca, L.; Francesca, C.; Daniela, G.; Alfredo, S.G.; Giuseppe, S. Cephalometric analysis of dental and skeletal effects of Carriere Motion 3D appliance for Class II malocclusion. *Am J Orthod Dentofacial Orthop* **2022**, *161*, 659–665. https://doi.org/10.1016/j.ajodo.2020.12.024.
34. Malinowski, K.; Chodur, M.; Majewski, M.; Malinowski, J. Age dependent treatment response to the Carriere Motion 3D appliance for the correction of Class II malocclusion. *Journal of Education, Health and Sport* **2022**, *12*, 169–177.
35. Nercellas Rodriguez, A.; Colino Gallardo, P.; Zubizarreta-Macho, A.; Colino Paniagua, C.; Alvarado Lorenzo, A.; Albaladejo Martinez, A. A New Digital Method to Quantify the Effects Produced by Carriere Motion Appliance. *J. Pers. Med.* **2023**, *13*.
36. Rodriguez, H.L. Long-Term Stability of Two-Phase Class II Treatment with the Carriere Motion Appliance. *J Clin Orthod* **2019**, *53*, 481–487.
37. Wilson, B.; Konstantoni, N.; Kim, K.B.; Foley, P.; Ueno, H. Three-dimensional cone-beam computed tomography comparison of shorty and standard Class II Carriere Motion appliance. *Angle Orthod* **2021**, *91*, 423–432. https://doi.org/10.2319/041320-295.1.

Preprints.org (www.preprints.org) | NOT PEER-REVIEWED | Posted: 6 February 2024 doi:10.20944/preprints202401.2047.v2

38. Areepong, D.; Kim, K.B.; Oliver, D.R.; Ueno, H. The Class II Carriere Motion appliance. *Angle Orthod* **2020**, *90*, 491–499. https://doi.org/10.2319/080919-523.1.
39. Fouda, A.S.; Attia, K.H.; Abouelezz, A.M.; El-Ghafour, M.A.; Aboulfotouh, M.H. Anchorage control using miniscrews in comparison to Essix appliance in treatment of postpubertal patients with Class II malocclusion using Carriere Motion Appliance. *Angle Orthod* **2022**, *92*, 45–54. https://doi.org/10.2319/021421-126.1.
40. Clermont, A.; Albert, A.; Bruwier, A. Effects of the Class II Carriere motion appliance in phase I treatment: A randomized controlled trial. *J Clin Orthod* **2022**, *56*, 285–293.
41. Areepong, D.; Kim, K.B.; Oliver, D.R.; Ueno, H. The Class II Carriere Motion appliance. *Angle Orthod* **2020**, *90*, 491–499. https://doi.org/10.2319/080919-523.1.
42. Fouda, A.S.; Aboulfotouh, M.H.; Attia, K.H.; Aboulezezz, A.M. Carriere Motion Appliance with Miniscrew Anchorage for Treatment of Class II, Division 1 Malocclusion. *J Clin Orthod* **2020**, *54*, 633–641.
43. Barakat, D.; Bakdach, W.M.M.; Youssef, M. Treatment effects of Carriere Motion Appliance on patients with class II malocclusion: A systematic review and meta-analysis. *Int Orthod* **2021**, *19*, 353–364. https://doi.org/10.1016/j.ortho.2021.05.005.
44. Lombardo, L.; Cremonini, F.; Oliverio, T.; Cervinara, F.; Siciliani, G. Class II correction with Carriere Motion 3D Appliance and clear aligner therapy. *J Clin Orthod* **2022**, *56*, 187–193.
45. Attia, KH; Aboulfotouh, M.F.A. Three-dimensional computed tomography evaluation of airway changes after treatment with Carriere Motion 3D Class II appliance. *J Dent Maxillofacial Res.* **2019**, *2*, 16–19.
46. Kim-Berman, H.; McNamara, JA, J.; JP, L.; McMullen, C.; Franchi, L. Treatment effects of the Carriere Motion 3D appliance for the correction of Class II malocclудion in adolescents. *Angle Orthod.* **2019**, *89*, 839–846.
47. Nasef, A; Refai, W. Application of a New Three Dimensional Method of Analysis for Comparison between the Effects of Two Different Methods of Distalisation of the Maxillary First Molar. *Egypt Dent J* **2015**, *61*, 4195–4201.
48. Hashem, A.S. Thre dimensional assessment of the long-term treatment stability after maxillary first molar distalisation with Carriere distalizer appliance. *Life Sci J* **2020**, *17*, 83–90.
49. Yin, K.; Han, E.; Guo, J.; Yasumura, T.; Grauer, D.; Sameshima, G. Evaluating the treatment effectiveness and efficiency of Carriere Distalizer: a cephalometric and study model comparison of Class II appliances. *Prog Orthod* **2019**, *20*, 24. https://doi.org/10.1186/s40510-019-0280-2.
50. Thurzo, A.; Urbanová, W.; Novák, B.; Waczulíková, I.; Varga, I. Utilization of a 3D Printed Orthodontic Distalizer for Tooth-Borne Hybrid Treatment in Class II Unilateral Malocclusions. *Materials* **2022**, *15*, 1740. https://doi.org/10.3390/ma15051740.
51. Deng, W.; Xie, D.; Liu, F.; Zhao, J.; Shen, L.; Tian, Z. DLP-Based 3D Printing for Automated Precision Manufacturing. *Mobile information systems* **2022**, *2022*, 1–14. https://doi.org/10.1155/2022/2272699.
52. liqcreate. Explained & tested: Anti-Aliasing (AA) and Blur in resin 3D-printing, 2023.
53. Federici Canova, F.; Oliva, G.; Beretta, M.; Dalessandri, D. Digital (R)Evolution: Open-Source Softwares for Orthodontics. *Appl. Sci.* **2021**, *11*.
54. Formlabs Form 3B+ printer. https://media.formlabs.com/m/759db40c7c05b049/original/-ENUS-Form-3B-manual.pdf.
55. Sarker, S.; Colton, A.; Wen, Z.; Xu, X.; Erdi, M.; Jones, A.; Kofinas, P.; Tubaldi, E.; Walczak, P.; Janowski, M.; et al. 3D-Printed Microinjection Needle Arrays via a Hybrid DLP-Direct Laser Writing Strategy. *Advanced materials technologies* **2023**, *8*, n/a. https://doi.org/10.1002/admt.202201641.
56. Form Wash Manual. https://media.formlabs.com/m/11c8523a56138d6/original/-ENUS-Form-Wash-Manual.pdf.
57. Form Cure Time and Temperature Settings. https://s3.amazonaws.com/servicecloudassets.formlabs.com/media/Finishing/Post-Curing/115001414464-Form%20Cure%20Time%20and%20Temperature%20Settings/FormCurePost-CureSettings.pdf.
58. Espinar-Escalona, E.; Barrera-Mora, J.M.; Llamas-Carreras, J.M.; Solano-Reina, E.; Rodriguez, D.; Gil, F.J. Improvement in adhesion of the brackets to the tooth by sandblasting treatment. *J Mater Sci Mater Med* **2012**, *23*, 605–11. https://doi.org/10.1007/s10856-011-4509-y.
59. Scribante, A.; Gallo, S.; Turcato, B.; Trovati, F.; Gandini, P.; Sfondrini, M.F. Fear of the Relapse: Effect of Composite Type on Adhesion Efficacy of Upper and Lower Orthodontic Fixed Retainers: In Vitro Investigation and Randomized Clinical Trial. *Polymers (Basel)* **2020**, *12*. https://doi.org/10.3390/polym12040963.

 doi:10.20944/preprints202401.2047.v2

60. Yilmaz, B.; Kara, M.; Seker, E.; Yenidunya, D. Do we know how much force we apply with latex intermaxillary elastics? *Apos Trends in Orthodontics* **2021**, *11*, 191–197.
61. Castroflorio, T.; Sedran, A.; Spadaro, F.; Rossini, G.; Cugliari, G.; Quinzi, V.; Deregibus, A. Analysis of Class II Intermaxillary Elastics Applied Forces: An in-vitro Study. *Frontiers in Dental Medicine* **2022**, *2*.
62. Saccomanno, S.; Quinzi, V.; Paskay, L.; Caccone, L.; Rasicci, L.; Fani, E.; Di Giandomenico, D.; Marzo, G. Evaluation of the Loss of Strength, Resistance, and Elasticity in th Different Types of Intraoral Orthodontic Elastics (IOE): A Systematic Review of the Literature of In Vitro Studies. *J. Pers. Med.* **2023**, *13*.
63. Dubovska, I.; Lickova, B.; Voborna, I.; Urbanova, W.; Kotova, M. Force of Intermaxillary Latex Elastics from Different Suppliers: A Comparative In Vitro Study. *Appl. Sci.* **2023**, *13*.
64. Medit Link Software. https://www.meditlink.com/home.
65. Stefanelli, L.; Franchina, A.; Pranno, A.; Pellegrino, G.; Ferri, A.; Pranno, N.; Di Carlo, S.; De Angelis, F. Use of Intraoral Scanners for Full Dental Arches; Could Different Strategies or Overlapping Software Affect Accuracy. *Int. Journal of Environmental Research and Public Health* **2021**, *18*, 13.
66. Martel, D. The Carriere Distalizer: simple and efficient. *Int J Orthod Milwaukee* **2012**, *23*, 63–6.